

^algarciap@ecc.edu.co

^bUniversidad ECCI, Cra. 19 No. 49-20, Bogotá, Colombia, Código Postal 11131

^cObservatorio Astronómico Nacional, Universidad Nacional de Colombia

ARTICLE INFO

Keywords:
 Cosmological parameters
 Dark Energy
 RCM 08.80.-k95.36.+x97.60.Bw

ABSTRACT

Observational constraints (EDE) on the evolution of the dark energy equation of state parameter $w(z)$ are studied in the context of the Λ CDM model. We consider a general form for $w(z)$ and use the latest observational data from the Supernova Legacy Survey, the Baryon Acoustic Oscillations (BAO) data from the Sloan Digital Sky Survey (SDSS), and the Cosmic Microwave Background (CMB) data from the Planck satellite. The constraints are compared with those obtained from the Λ CDM model. The results show that the EDE model is favored over the Λ CDM model at the 95% confidence level. The best-fit parameters are $w_0 = -1.0$ and $w_1 = 0.1$. The evolution of $w(z)$ is shown to be consistent with the Λ CDM model at low redshifts but deviates significantly at high redshifts. The constraints on the parameters of the EDE model are also compared with those obtained from other observational data sets. The results show that the EDE model is favored over the Λ CDM model at the 95% confidence level. The best-fit parameters are $w_0 = -1.0$ and $w_1 = 0.1$. The evolution of $w(z)$ is shown to be consistent with the Λ CDM model at low redshifts but deviates significantly at high redshifts.

1. Introduction

The discovery of the accelerating expansion of the universe (SNIa, Riess et al., 2000) has led to the introduction of the dark energy component in the cosmological model. The dark energy is characterized by its equation of state parameter w , which is defined as the ratio of its pressure to its energy density. The Λ CDM model, which assumes a constant equation of state parameter $w = -1$, is the standard model of cosmology. However, there are several observational constraints that challenge the Λ CDM model. In particular, the evolution of the dark energy equation of state parameter $w(z)$ is a key feature of the dark energy model. The evolution of $w(z)$ is constrained by observational data sets such as the Supernova Legacy Survey (SLS), the Baryon Acoustic Oscillations (BAO) data from the Sloan Digital Sky Survey (SDSS), and the Cosmic Microwave Background (CMB) data from the Planck satellite. The constraints on the parameters of the EDE model are also compared with those obtained from other observational data sets. The results show that the EDE model is favored over the Λ CDM model at the 95% confidence level. The best-fit parameters are $w_0 = -1.0$ and $w_1 = 0.1$. The evolution of $w(z)$ is shown to be consistent with the Λ CDM model at low redshifts but deviates significantly at high redshifts.

(SLS; Riess et al., 2000; Kim et al., 2020), the Λ CDM model is the standard model of cosmology. However, there are several observational constraints that challenge the Λ CDM model. In particular, the evolution of the dark energy equation of state parameter $w(z)$ is a key feature of the dark energy model. The evolution of $w(z)$ is constrained by observational data sets such as the Supernova Legacy Survey (SLS), the Baryon Acoustic Oscillations (BAO) data from the Sloan Digital Sky Survey (SDSS), and the Cosmic Microwave Background (CMB) data from the Planck satellite. The constraints on the parameters of the EDE model are also compared with those obtained from other observational data sets. The results show that the EDE model is favored over the Λ CDM model at the 95% confidence level. The best-fit parameters are $w_0 = -1.0$ and $w_1 = 0.1$. The evolution of $w(z)$ is shown to be consistent with the Λ CDM model at low redshifts but deviates significantly at high redshifts.

Statefinder $\{s, r\}$ Λ CDM ρ_{de} ω_{de} $H(z)$ $z \sim 10^{11}$ $\rho_{de|rad} = b \cdot \rho_{rad}$ $0 \leq b < 1$. (1)

$\rho_{rad} \propto a^{-4}$. Asa

$\Omega_{0m} = 0.3111 \pm 0.0056$, $\Omega_{\Lambda} = 0.6889 \pm 0.0056$ $H_0 = 67.66 \pm 0.42 \text{ km s}^{-1} \text{ Mpc}^{-1}$ ($h = 0.6766$), Λ CDM

Λ CDM ω_{de} Λ , ω_{de} m z_* $z_{eq} + z_{de}$ z_{de}

2. Effective parametrization of ω_{ϕ}

Λ CDM ρ_{ϕ} $-1 < \omega_{de} < -\frac{1}{3}$. Asa Λ Λ CDM ρ_{ϕ}

$H(z)$, $z \sim 10^{11}$ $\rho_{de|rad} = b \cdot \rho_{rad}$ $0 \leq b < 1$. (1)

$\rho_{de|rad} \propto a^{-4}$. Asa

Diff Λ CDM ω_{de} Λ , ω_{de} m z_* $z_{eq} + z_{de}$ z_{de}

$$\omega_{\phi}(z) = \frac{4/3}{\left(\frac{1+z_*}{1+z}\right)^m + 1} - 1. \tag{2}$$

$$z_* = \frac{z_{eq} + z_{de}}{2} \tag{3}$$

Λ CDM ρ_{ϕ}

$$\int_{\rho}^{\rho_0} \frac{d\rho'}{\rho'} = -3 \int_a^1 \frac{(1 + \omega_{\phi}(a'))}{a'} da', \tag{4}$$

(4), ρ_{ϕ}

$$\rho = \rho_0 \cdot (1+z)^4 \left[\frac{\left(\frac{1+z_*}{1+z}\right)^m + 1}{(1+z_*)^m + 1} \right]^{4/m} = \rho_0 \cdot f(z). \tag{5}$$

iv

$$f(z) = (1+z)^4 \left[\frac{\left(\frac{1+z_*}{1+z}\right)^m + 1}{(1+z_*)^m + 1} \right]^{4/m}. \quad (6)$$

Modeling

$$F = \frac{\rho_\phi}{\rho_{cr}}$$

$$\Omega_\phi = 1 -$$

$$\Omega_\phi(z) = \frac{\rho_0}{\rho_c} = \frac{\Omega_{\phi 0} \cdot f(z)}{\Omega_{\phi 0} \cdot f(z) + \Omega_{m 0} \cdot (1+z)^3}. \quad (7)$$

Observational

$$\Omega_{\phi 0} + \Omega_{m 0} + \Omega_{d 0} = 1 \quad \Omega_{d 0} \rightarrow 0$$

$$\Omega_{\phi 0} + \Omega_{m 0} + \Omega_{d 0} =$$

3. Best fitting parameters of the model

Best fit (2) is

$$\{\Omega_{\phi_0}, m, z_{de}\},$$

where

the best fit

is obtained

by minimizing

the chi-squared

statistic

using

$$m \text{ and } z_{de}$$

using

(S.P.1 et al., 2014)

and R_{CMB}

is

defined

as

$$z = z_{de}. \text{ At}$$

$$R_{CMB} \text{ is}$$

MCMC

analysis

is

$$\Omega_{\phi_0}$$

is

$$[0, 1] \text{ and}$$

$$N_{\phi}$$

is

$$m$$

is fixed

at

$m = 0$

and

$m > 90$

is

fixed

at

$m = 90$

and

m

is

fixed

at

$m = 90$

and

m

• The

best fit

parameters

are

Ω_{ϕ_0}

m

z_{de}

and

R_{CMB}

z_{de}

$$\Rightarrow 0 < z_{de} \lesssim 1.5.$$

DFGR², 6DFGS³, WIGGLEZ⁴ and

SDSS

data

are

used

to

fit

the

model

parameters

are

Ω_{ϕ_0}

m

z_{de}

and

R_{CMB}

is

defined

as

R_{CMB}

is

defined

as

R_{CMB}

is

defined

as

R_{CMB}

is

defined

as

R_{CMB}

is

defined

as

R_{CMB}

is

defined

as

R_{CMB}

is

defined

as

R_{CMB}

is

defined

as

R_{CMB}

is

defined

as

R_{CMB}

is

defined

$$d_L(z) = \frac{c(1+z)}{H_0} \int_0^z \frac{dz'}{B(z')}, \quad (8)$$

$$B(z') = (\Omega_{\phi_0} f(z'; m, z_*) + (1 - \Omega_{\phi_0})(1+z')^3)^{1/2},$$

$$\mu = m - M = 5(\log_{10} d_L(z) - 1). \quad (9)$$

As the CMB

is

fixed

at

R_{CMB}

is

defined

as

R_{CMB}

is

defined

as

R_{CMB}

is

defined

as

R_{CMB}

is

defined

as

R_{CMB}

is

defined

as

R_{CMB}

is

defined

as

R_{CMB}

is

defined

as

R_{CMB}

is

defined

as

R_{CMB}

is

²<http://www.2dfgrs.net/>

³<http://www.6dfgs.net/>

⁴<http://wigglez.swin.edu.au/>

⁵<https://www.sdss.org/>

¹<http://www.supernova.lbl.gov/>

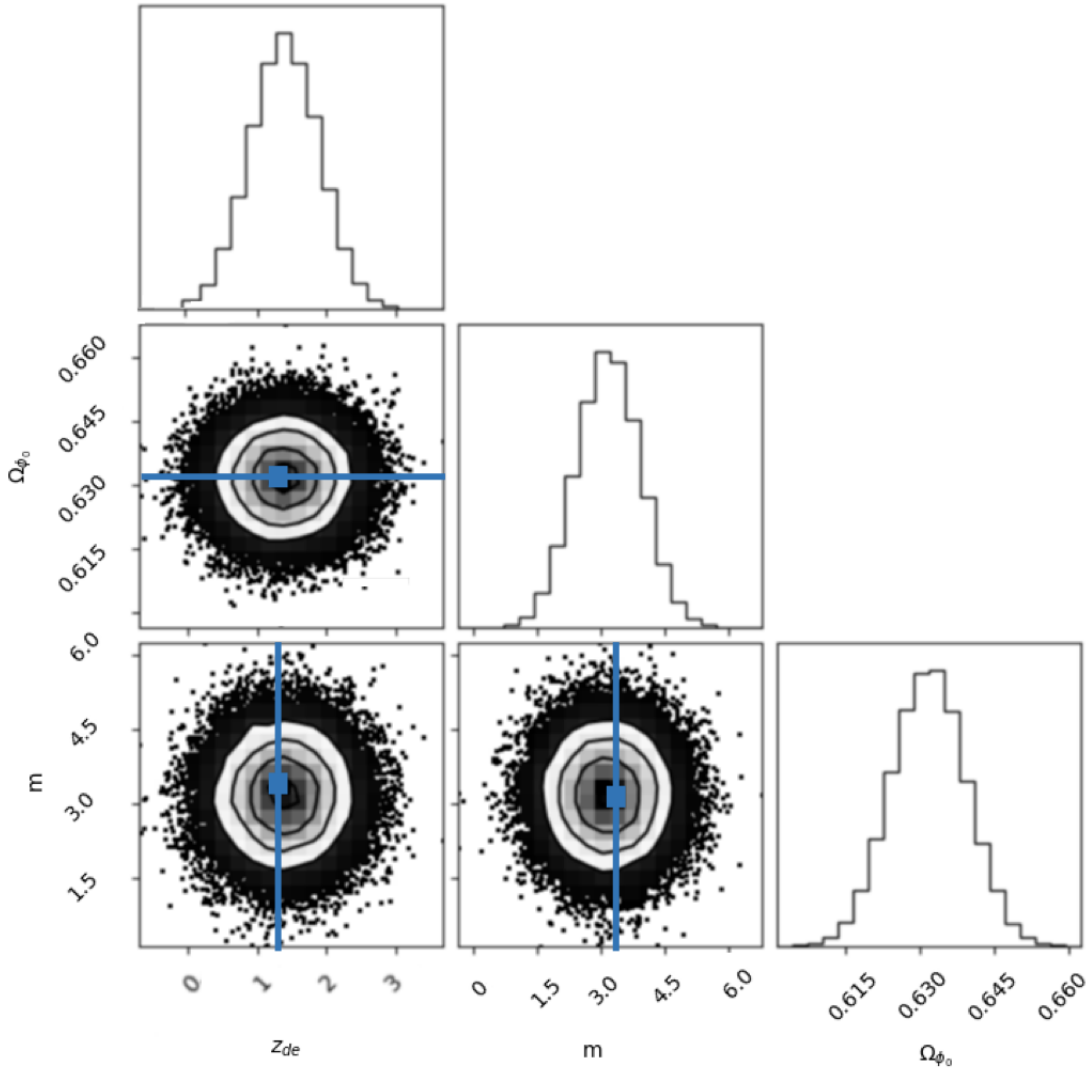


Figure 1: Posteriors of our free parameters Ω_{ϕ_0} , m and z_{de} , with shaded 68% intervals, fitting to SNIa luminosity distances data from SCP2.1, on top of the simultaneous constraints given by the CMB shift parameter R_{CMB} and the deceleration parameter $q(z_{de}) = 0$. The best values estimated with the MCMC method lay within the prior conditions. With our analysis, we are able to recover the best values of the free parameters: $\Omega_{\phi_0} = 0.63 \pm 0.05$, $m = 3.2 \pm 0.9$, and $z_{de} = 1.2 \pm 0.3$. The latter parameters maximize the likelihood function, and break the tight degeneracy existent between m and z_{de} .

$q(z_{de}) = 0$ in $q(z) = (1+z)\frac{\partial H}{\partial z} - 1$. (11)

We use MCMC to fit the parameters Ω_{ϕ_0} , m , and z_{de} . The best-fit values are $\Omega_{\phi_0} = 0.63 \pm 0.05$, $m = 3.2 \pm 0.9$, and $z_{de} = 1.2 \pm 0.3$. The shaded regions in the corner plot represent the 68% confidence intervals.

The CMB shift parameter R_{CMB} is defined as $R_{\text{CMB}} = \frac{H(z_{\text{CMB}}) D_{\text{CMB}}}{H_0 D_{\text{CMB}}}$, where $H(z)$ is the Hubble parameter and D_{CMB} is the comoving distance to the CMB.

Table 1

Summary of the best values of the free parameters of the DE model and comparison with the Λ CDM. Column 1: parameter name. Column 2: estimates for our model. Column 3: Λ CDM comparison (Planck Collaboration et al., 2018).

Parameter	Our model	Λ CDM model
Ω_{ϕ_0}	0.631 ± 0.005	0.6889 ± 0.0056
m	3.2 ± 0.9	–
z_{de}	1.2 ± 0.3	–
Ω_{m_0}	0.369 ± 0.005	0.3111 ± 0.0056
ω_0	-0.976 ± 0.358	-1

rich (2018),

4. Evolution of the observables associated to the DE model

MCMC

Fig 2

Fig 4

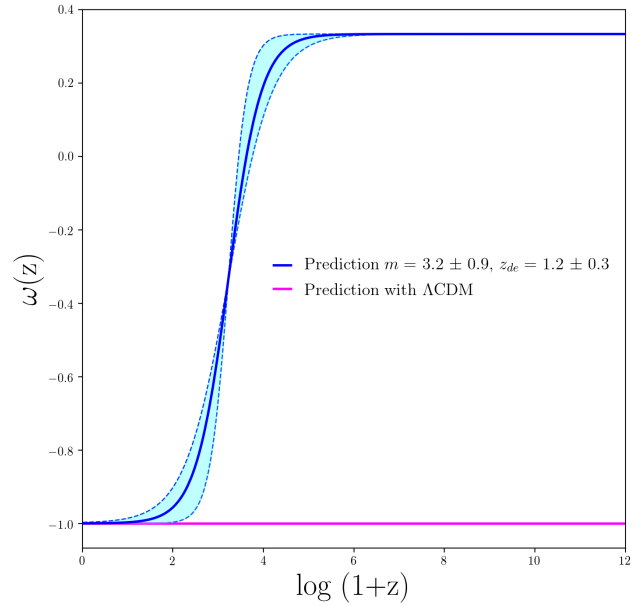


Figure 2: Equation of state $\omega(z)$ as a function of redshift z . The parameterization is valid up to the Planck time. The blue line represents the equation of state of the field, the dashed lines show the upper and lower limits of $\omega(z)$, whereas the cyan region displays all the possible values that the equation of state could take inside the parameter-space allowed within the error bars. The purple line shows a comparison of the evolution of the equation of state in the case of the Λ CDM model.

Model

Fig 5

ACDM

ACDM

$z \sim 1$

ACDM

MAP

H_0

Fig 6

Ly

α

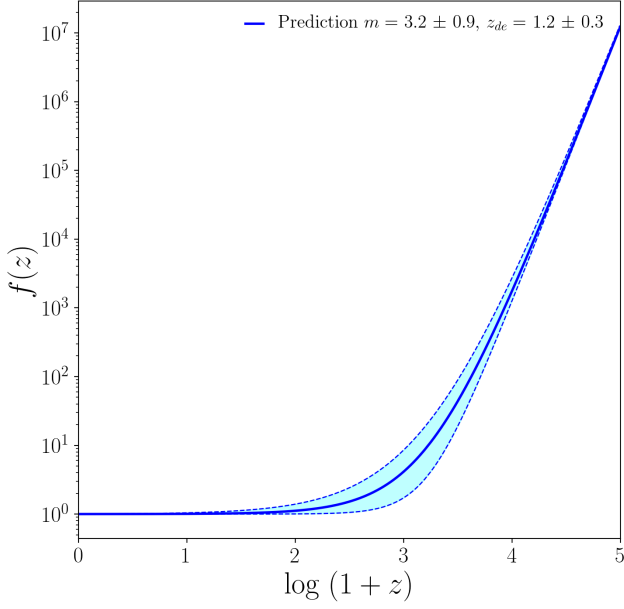


Figure 3: Dark energy density factor $f(z)$ as a function of redshift z . The factor grows with redshift, differently from the evolution of the dark energy density Ω_ϕ . The blue continuous line shows the evolution of $f(z)$, whereas the dashed lines the upper and lower limits of the function inside the error bars of the parameters. The cyan shaded region, all the possible values of $f(z)$ within the parameter-space.

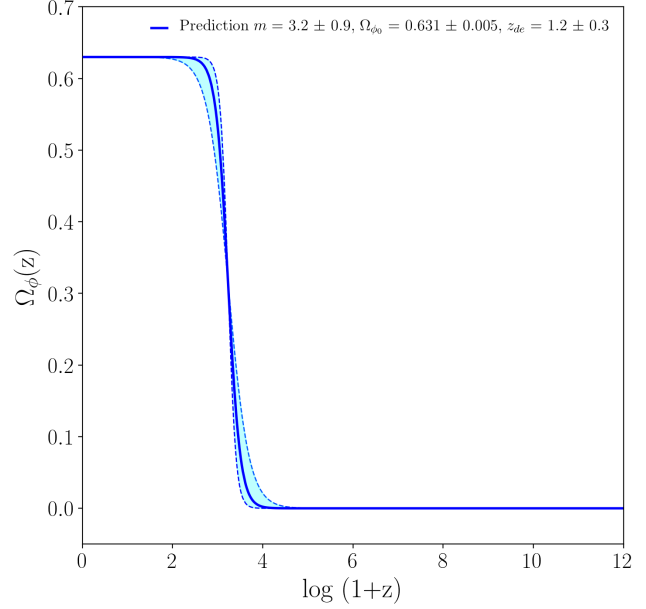


Figure 4: Dark energy density fraction Ω_ϕ with redshift z . The blue line presents the evolution of the energy density of the field. The dashed lines show the upper and lower limits of the dark energy density inside the error bars of the parameters. Within these boundaries, in the cyan shaded region, the possible values of Ω_ϕ within the parameter-space. It is worth noticing that at $z \sim 10^{10}$, Ω_ϕ raises from a value close to zero, indicating that our model is an EDE and its energy density fraction could contribute with some effective degrees of freedom in the Hubble parameter at radiation domination era.

the Planck (2019) in
the Λ CDM
Chen (2018) in
the Λ CDM
the Planck (2019) in
the Λ CDM

5. Standard Cosmological Probes

Age of the Universe with this model

the Planck (2019)
the Λ CDM

$$t_0 = \frac{1}{H_0} \int_0^\infty \frac{dz'}{(1+z') \sqrt{\Omega_{\phi 0} \cdot f(z) + \Omega_{m 0} \cdot (1+z)^3}}, \quad (12)$$

the Planck (2019),
the Λ CDM

$$t_0 = 13.441 \pm 0.004 \text{ Gy} . \quad (13)$$

As can be seen from
eq.(13) the
the Planck (2019)
the Λ CDM
the Planck (2019)
the Λ CDM

the Planck (2019)
the Λ CDM
the Planck (2019)
the Λ CDM
the Planck (2019)
the Λ CDM
the Planck (2019)
the Λ CDM
the Planck (2019)
the Λ CDM

Statefinder parameters

the Planck (2019)
the Λ CDM, the
Statefinder

$$r = 1 + \frac{9}{2} \Omega_\phi \omega_\phi (1 + \omega_\phi) - \frac{3}{2} \Omega_\phi \frac{\dot{\omega}_\phi}{H}, \quad (14)$$

$$s = 1 + \omega_\phi - \frac{1}{3} \frac{\dot{\omega}_\phi}{H \omega_\phi}, \quad (15)$$

the Planck (2019)
{r, s} = {1, -1} in
the Λ CDM,
the Planck (2019)
the Λ CDM
the Planck (2019)
the Λ CDM

Statefinder parameters

the Planck (2019)
the Λ CDM and DE
{r, s} = {0, 0} in
r > 0

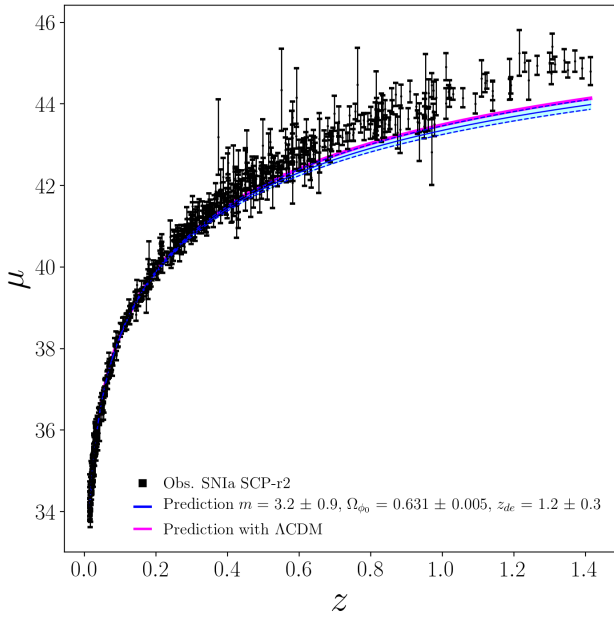


Figure 5: Distance modulus vs. redshift z computed with our model and Λ CDM. We compare the theoretical predictions with observational data of SNIa from SCP2.1. We present our model, Λ CDM and SNIa from SCP release in the blue line, magenta line and black points, respectively.

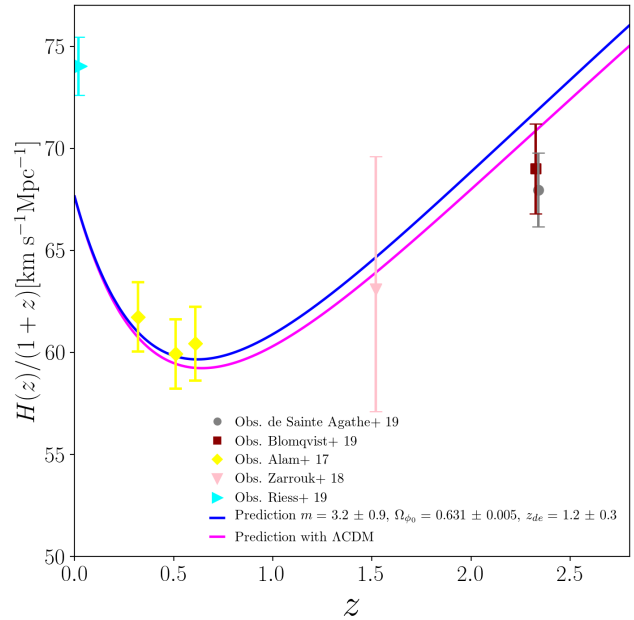


Figure 6: Prediction for $H(z)/(1+z)$ as a function of z . We compare our model (blue solid line) with Λ CDM model (magenta solid line) and BAO observations derived with BOSS DR12 from Alam et al. (2017) in yellow diamonds, from BOSS DR14 quasars by Zarrouk et al. (2018) in the pink inverted triangle, BOSS DR14 Ly α autocorrelation at $z = 2.34$ with the grey circle, and BOSS DR14 joint constraint from the Ly α auto-correlation and cross-correlation with quasars from Blomqvist et al. (2019) in the dark red square. All the previous observations have computed with Planck Collaboration et al. (2018) cosmological parameters. The inferred Hubble measurement at $z = 0$ derived independently by Riess et al. (2019) is shown with the cyan right tilted triangle.

$s < 0$). $\Omega_{\phi 0}$ $\omega_{\phi} = -1$ Λ CDM, $\Omega_{m0}, \Omega_{\phi 0}$ z_* Λ CDM

6. Conclusions and perspectives

... $z \sim 1.4$ R_{CMB} $z = z_{de}$ $\Omega_{\phi 0}$ m

z_{de} $\omega(z)$

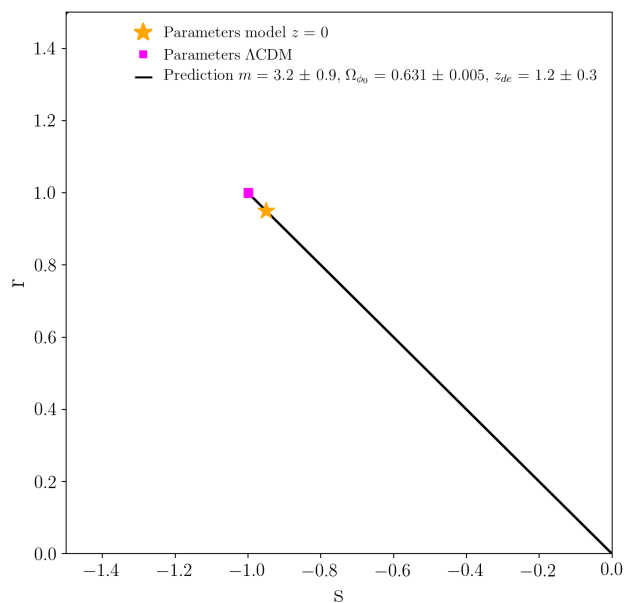


Figure 7: *Statefinder* parameters space. The set of parameters today for Λ CDM is presented with a purple square $\{r, s\} = \{1, -1\}$, while the values for our DE model are shown with the golden star. The black line exhibits the evolution with redshift of the *Statefinder* parameters given our model. The effective parametrization evolves from high redshift (early times) in the right lower side to the future in the left upper corner.

Statefinder parameters space

Function

Λ , function

$$\rho_{de}(z) = \rho_{de0} \exp \left[\int_0^z \frac{3}{1+z'} (1 + \omega(z')) dz' \right]$$

Acknowledgments

L.A. García et al.

References

Abbott et al. (2017) *Planck 2015 results. XII. Cosmological parameters*

Ahmed, B. H., & G. G., 1948. *MNRAS* 8, 383–384.

Akiyama, C., & M. Y. 1999. *Phys Rev D* 60, 083519. arXiv:hep-th/9904075.

Ash, C., & M. V. 2001. *Phys Rev D* 63, 103510. arXiv:astro-ph/0006373.

Baugh, M. C., & B. A. A., 2004. *MNRAS* 349, 1085–1109. arXiv:astro-ph/0407239.

Bell, M., & B. H., & B. N. G., et al. 2019. *Phys Rev D* 100, 103511. arXiv:1904.03430.

Binetruy, J., & M. G., 1997. *Phys Rev D* 55, 23–29. arXiv:astro-ph/9702100.

Carr, S. C., & A. C., 2002. *Phys Rev D* 66, 063514. arXiv:astro-ph/0206298.

Chen, Y., & J. M. 2011. *Phys Rev D* 83, 3. arXiv:1002.4928.

Chen, Y., & J. M., 2006. *Phys Rev D* 73, 023511.

Chen, Y., & J. M., 2012. *Phys Rev D* 86, 113001. arXiv:1106.2476.

Chen, Y., & J. M., 2004. *Phys Rev D* 70, 043543. arXiv:hep-ph/0311312.

Das, R., & M. M., 2018. *Phys Rev D* 97, 123525.

DeFelice, A., & S. 2010. *Phys Rev D* 81, 3. arXiv:1002.4928.

Dodelson, M., & G., 2006. *Phys Rev D* 73, 023511.

Elgar, B. J. R. 1999. *Phys Rev D* 60, 103511. arXiv:astro-ph/9807103.

Farr, Y., & C. S. 2011. *Phys Rev D* 83, 3. arXiv:1002.4928.

Guth, A. H., 1996. *Phys Rev D* 53, 2435–2450.

Guo, X., & R., 2010. *Phys Rev D* 81, 083501. arXiv:1003.2786.

Guth, A. H., 1981. *Phys Rev D* 23, 347–356.

Guth, A. H., 2000. *Phys Rev D* 62, 043526. arXiv:hep-th/0004008.

Hellmuth, P., & D., 2000. *Phys Rev D* 61, 123525. arXiv:hep-th/0001145.

Hughes, K., & S., 2015. *Phys Rev D* 91, 023511. arXiv:1509.00969.

Kahn, A., & M. U. Y. 2000. *Phys Rev D* 61, 083501. arXiv:gr-qc/0005011.

Kobayashi, M., & B. C., & A. M., 2020. *Phys Rev D* 101, 103511. arXiv:2001.10252.

Liu, C. S., & A. B. D., 2017. *Phys Rev D* 95, 083501.

043510. arXiv:1706.00730.
 P.G., 2011. *Astrophys. J.* **733**, 3191–3199.
 arXiv:1107.4475.
 P.P., R.B., 2003. *Phys. Rev. D* **67**, 559–606. arXiv:astro-ph/0207347.
 P.A.R. Adkins, A.M. Abad, M., A.J., B.C., B.A.J., B.B., B.J.G., et al. 2015. *MNRAS* **451**, 1–11. arXiv:1502.01589.
 P.A.R. Adkins, A.M. Abad, et al. 2018. *MNRAS* **475**, 1–11. arXiv:1807.06209.
 P.P., P.E., 1988. *Phys. Rev. D* **37**, 3406–3427.
 P.A.G., C.S. Adkins, L.M., S.D., 2019. *MNRAS* **481**, 1–11. arXiv:1903.07603.
 P.A.G., F.A. et al. 2000. *Phys. Rev. D* **62**, 62–67. arXiv:astro-ph/0001384.
 P.D., A.G.S. et al. 2014. *MNRAS* **441**, 223–245.
 P.M., T. 2003. *Phys. Rev. D* **67**, 083509. arXiv:hep-th/0212317.
 P.A., 2002a. *Phys. Rev. D* **65**, 048. arXiv:hep-th/0203211.
 P.A., 2002b. *Phys. Rev. D* **65**, 065. arXiv:hep-th/0203265.
 P.C., 2004. *Phys. Rev. D* **69**, 17–22.
 P.P. B.E., G.M. H. et al. 2018. *MNRAS* **474**, 1639–1663. doi:10.1093/mnras/sty506, arXiv:1801.03062.